buildings

MDPI

Article

Load Distribution Optimization of Steel Storage Rack Based on Genetic Algorithm

Tianyang Deng [1], Yu Niu [1], Lingfeng Yin [1,2,*], Zhiqiang Lin [1] and Zhanjie Li [3]

[1] School of Civil Engineering, Southeast University, Nanjing 211189, China
[2] School of Engineering, Tibet University, Lhasa 850011, China
[3] Department of Engineering, SUNY Polytechnic Institute, Utica, NY 13502, USA
* Correspondence: eking@seu.edu.cn; Tel.: +86-139-5191-7218

Abstract: The distribution of load has high uncertainty, which is the main cause of a rack structure's instabilities. The objective of this study was to identify the most unfavorable and favorable load distributions on steel storage racks with and without bracings under seismic loading through a stochastic optimization—a genetic algorithm (GA). This paper begins with optimizing the most unfavorable and favorable load distributions on the steel storage racks with and without bracings using GA. Based on the optimization results, the failure position and seismic performance influencing factors, such as the load distributions on the racks and at hazardous positions, are then identified. In addition, it is demonstrated that the maximum stress ratio of the uprights under the most unfavorable load distribution is higher than that under the full-load normal design, and it is not the case that the higher the center of gravity the more dangerous the steel storage rack is, demonstrating that the load distribution pattern has a significant impact on the structural safety of steel storage racks. The statistics of the distributions of the load generated during the optimization of the GA and the contours of the probability distributions of the load are generated. Combining the probability distribution contours and the GA's optimization findings, the "convex" distribution hazard model and the "concave" distribution safety model for a steel storage rack with bracings are identified. In addition, the features of the distribution hazard model and the load distribution safety model are also identified for steel storage racks without bracings.

Keywords: steel storage rack; seismic design; genetic algorithm; load distribution pattern

Citation: Deng, T.; Niu, Y.; Yin, L.; Lin, Z.; Li, Z. Load Distribution Optimization of Steel Storage Rack Based on Genetic Algorithm. *Buildings* **2022**, *12*, 1782. https://doi.org/10.3390/buildings12111782

Academic Editors: Wenying Zhang, Ziqin Jiang and Shaole Yu

Received: 21 September 2022
Accepted: 21 October 2022
Published: 24 October 2022

1. Introduction

Steel storage racks play a critical role in the popularity of online shopping. At present, the research on steel storage racks mainly focuses on the structural performance of steel storage racks' members and components such as uprights [1–5], joints [6–13], and frames [14–17]. Typically, these investigations assume that the effects of the center of gravity and eccentricity of the load are disregarded. However, the weight of the load stored in the steel storage rack usually significantly exceeds the weight of the rack itself. When the steel storage rack is not fully loaded, the center of gravity and the eccentricity of the load have great influences on the seismic performance of the steel storage rack. Consequently, these conclusions may not be rigorous. In addition, the current anti-seismic design standards for racks generally consider that the loads are evenly distributed on the steel storage rack [18–20]. Therefore, investigating the potential impact of the distributions of the load on the seismic performance of the steel storage rack plays a critical role in improving the safety of the steel storage rack under an earthquake.

Previous research has suggested that the failure of a steel rack structural system, such as progressive dynamic collapse, is most likely caused by the fall of the pallets and the impact of loads on the structure at lower levels. The falling of pallets may endanger the lives of customers as well as workmen and employees, which involves not only the casualty

risk with potential legal concerns but also significant economic loss concerning insurance coverage [21]. Beale et al. [22] came to the conclusion that the loads could not simply be assumed to be distributed symmetrically in a non-linear analysis of steel storage racks. Following that, a finite element model of steel storage racks was developed [23]. The results revealed that the distribution of load under partial load is frequently the cause of structural failure of the rack. Qarud et al. [24] developed a six-level, six-bay, three-dimensional FE model of a steel storage rack using ABAQUS and performed multiple non-linear analyses on the steel storage rack under full or partial load. The study found that a steel storage rack under partial load is more dangerous than one under full load because only the steel storage rack under full load did not fail in the global sway mode. Simon et al. [25] investigated the effect of mass eccentricities on the seismic response of an existing externally braced steel frame high rack, specifically considering three different extreme load distributions. The results show that the most unfavorable load eccentricities may increase the risk under earthquakes and lead to local instability of the rack uprights. Hence, some studies in the past sought to identify these favorable or unfavorable load distributions using optimization methods such as a genetic algorithm (GA). A GA is a stochastic method to search the optimal solution by simulating the natural evolution process. It is a population-based search algorithm that exploits the concept of survival of the fittest [26]. Using a GA, Yang et al. [27] and Zhu et al. [28] have conducted optimization studies on steel storage racks. It was discovered that the optimized steel storage rack had a lower center of gravity and shorter access times.

The aforementioned studies revealed the potential risks of partially loaded racks. However, those experiments and numerical simulations [21–25] were limited and only reflected the relationship between several specific load distributions and the stability of steel storage racks. Investigating the relationship between load distribution and steel storage rack stability by increasing the number of test specimens or the number of finite element models requires significant financial or computational costs. Utilizing GAs and structural analysis software to optimize load distribution would be a fantastic strategy [27,28]. However, the optimization objective could not simply focus on the speculation that the lower the center of gravity is, the more stable the structure is. Whether this speculation is valid or not, more studies are warranted.

In this paper, steel storage racks under 60%, 70%, and 80% of full load are optimized using GA based on the seismic design method [29–31]. The optimization algorithm takes the stress ratio of the upright, which is calculated based on the Chinese technical code of cold-formed thin-walled steel structures (GB50018 [30]) and passed to SAP2000, as the objective function. Note, the analysis was conducted using the beam element formulated in SAP2000. With this implementation of the beam element—a six-degree beam element formulation—the warping effect is not accurately accounted in this analysis. Hence, the internal stress calculated here is only an approximation. However, from the strength calculation using GB50018, the global buckling, local buckling, warping, and their coupling are considered. The code, based on the theory of the effective width method, establishes a set of methods for calculating the bearing capacity and stress ratio of components with parameters such as the slenderness ratio. Moreover, the buckling states specified by the code are also utilized for the efficiency of the optimization. The most unfavorable and favorable load distributions are obtained from the optimization, and their commonalities are summarized. The effect of the load distribution on the seismic performance of the steel storage rack structure is evaluated. The load distribution methods generated during the optimization process are counted, and probability distribution contours are provided. According to the probability distribution contours and the GA optimization's findings, the hazardous and safe models of load distribution are generated for steel storage racks with and without bracings.

2. Development of Numerical Models

Tang et al. [32] investigated the effect of load distribution on the seismic performance of steel storage racks. Based on this research, two types of steel rack models with and without bracings were developed. The specifications of the components are shown in Table 1. The detailed dimensions of the components are shown in Figure 1. The front elevation, side elevation, upright section, and the corresponding geometric parameters of the model are shown in Figure 2.

Table 1. Model component specifications.

Component	Upright	Beams	Spine Bracing	Beams with Spine Bracing
Specification	Ω100 × 70 × 3	□100 × 50 × 1.5	C70 × 25 × 12 × 2	C70 × 25 × 12 × 2
Component	**Webs of upright frames**	**Longitude horizontal bracing**	**Bracing brackets**	**Plan bracing**
Specification	C40 × 29 × 6.5 × 1.3	C80 × 50 × 20 × 2.5	□60 × 50 × 2 × 2	□100 × 50 × 2.5 × 2.5

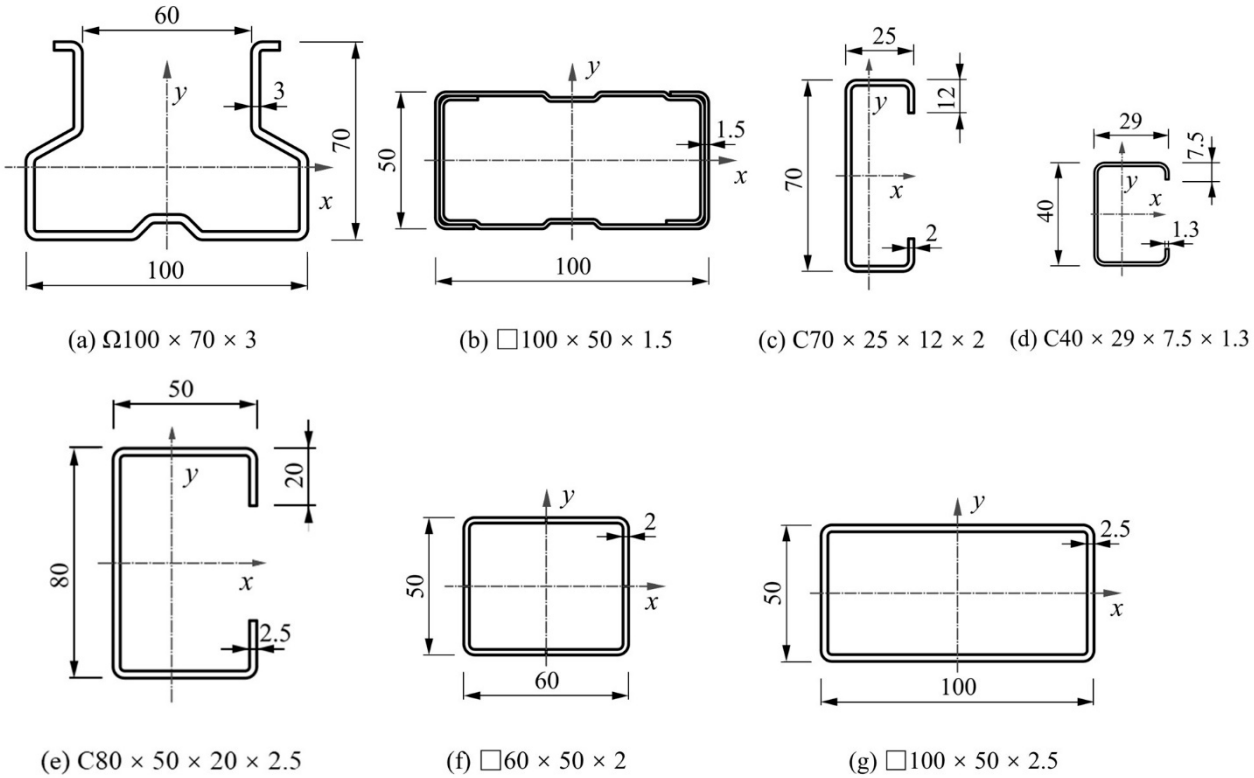

Figure 1. Detailed dimensions of the components.

Based on CECS23-1990 [29], the seismic fortification intensity is 8 degrees and site soil category is class II. Design earthquakes are grouped into the first group. The characteristic period of the site is 0.40 s. The design basic seismic acceleration is 0.2 g and the damping ratio is 0.05. The weight of each pallet is 10.8 kN. The live load distributed on the beam is 2.0 kN/m and the base-plate connections are defined as pinned connections, which is consistent with the previous study [32]. An experimental study has been reported by Yin et al. [6] on speed-lock connections in racks. In this paper, a normal and standard speed-lock connection studied by Yin et al. [6] is adopted, and the connection stiffness is 116.3 kN·m/rad. The steel used here is Q235 [33] steel with a nominal yield strength of 235 MPa, and the load combination taken into account in the strength-checking calculation is the same as the steel storage rack with bracings. When the rack is completely loaded, the

maximum stress ratio of the upright is 1.025 for the rack with bracings and 0.941 for the rack without bracings, which satisfies the standards of CECS23-1990 [29].

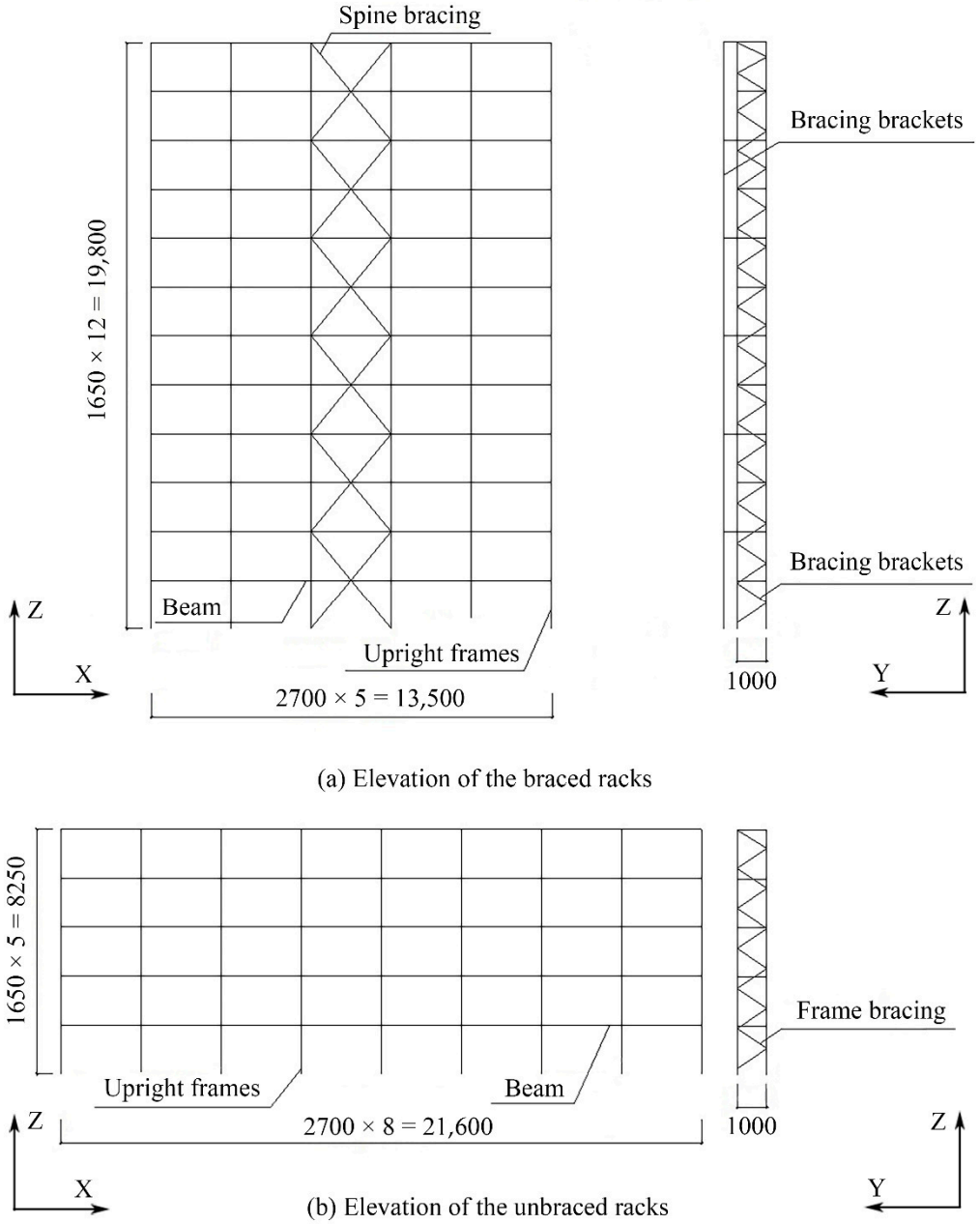

Figure 2. Detailed dimensions of the components (units: mm).

In this study, the center of gravity and the eccentricity of the model were defined. As shown in Figure 3, the center of gravity of the first level of load was set to 1, the center of gravity of the second level of load was set to 2, and so on. Therefore, the larger the sum of the centers of gravity of all the loads, the higher the loads were placed; and the smaller the sum, the lower the loads were placed. The eccentricities of the first row of load counted from both sides were set to 2 and −2, the second row were set to 1 and −1, and the middle row was set to 0. Therefore, the larger the absolute value of the sum of the eccentricities of all the loads, the larger the eccentricity of the load; and the smaller the absolute value of the sum, the smaller the eccentricity of the load. The center of gravity and the eccentricity of steel storage racks without bracings were set in the same way. Based on this model, the

overall height of the center of gravity H, the horizontal eccentricity distance P, and the total number of loads K of the steel storage rack can be calculated according to Equations (1)–(4).

$$K = \sum_{i=1}^{m} k_i \tag{1}$$

$$H = \sum_{i=1}^{m} k_i h_i / K \tag{2}$$

$$K = \sum_{j=1}^{n} k'_j \tag{3}$$

$$P = \sum_{j=1}^{n} k'_j p_j / K \tag{4}$$

where h_i is the height of the center of gravity of the i-th level of load, p_j is the eccentricity of the load in the j-th row, k_i is the number of loads in the i-th level, k'_j is the number of loads in the j-th row, and m and n correspond to the numbers of levels and rows of the steel storage rack, respectively.

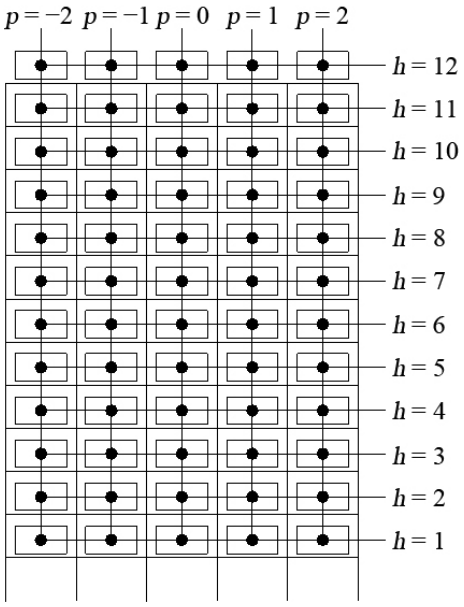

Figure 3. Diagram of the center of gravity and the eccentricity of steel storage racks with bracings.

3. Load Distribution Optimization Algorithm and Process

Numerous optimization issues in science and engineering can be partially resolved by the GA, at least for engineering application purposes [34]. In order to find the safest and most dangerous load distribution pattern, a GA, a global stochastic search method inspired by nature, is applied. It repeats the genetic operators of selection, crossover, and mutation to imitate biological replication and evolution. Modifications to the GA have been created to accommodate binary-coded and discrete data [35]. The essence of load position optimization is to establish a mapping between the load and positions. There is a one-to-many mapping link between the load and positions, given that a position can only hold one load. This study assumed that there were only two possibilities of no load and full load at each position for the purposes of the investigation. Based on the above assumptions, a binary code was used, with 1 indicating a full load position and 0 indicating an empty position. A chromosome represents a load position and its loading. The algorithm's code was represented as a string of 60-bit binary code, which corresponded

to the model's 60 positions. Based on the pre-designed 60%, 70%, and 80% of full load, 36, 42, and 48 code strings were set to 1, and the rest of the codes were set to 0. As shown in Figure 4, chromosome 1 represents that the load of position 1 is 0 (empty), and chromosome 2 represents that the load of position 2 is 1 (full), etc.

Chromosome (Positions, Load)								
Positions	1	2	3	4	5	6	……	60
Load	0	1	1	1	0	1	……	1

Figure 4. Schematic diagram of position code.

The program block diagram of the GA is shown in Figure 5 and the related parameters in the GA are shown in Table 2. In this study, GA optimization followed the classical algorithm flow. After inputting the necessary parameters, the fitness function of population genes is calculated. The $N_P \times T_a$ individuals with poor fitness will be eliminated in accordance with the set rules and proportions, while the remaining individuals with high fitness will be retained. The retained part is selected by roulette betting, and the gene coding is crossed and mutated to supplement the $N_P \times T_a$ eliminated individuals and form a new population. So far, a round of iterations of GA has been completed. When the number of iterations reaches the preset value N_G, the algorithm is terminated. Initialization, selection, crossover, and mutation of the population were realized by matrix operation in MATLAB. The fitness function was defined as the maximum stress ratio calculated by SAP2000, and the overall optimization was based on the interaction between the two software.

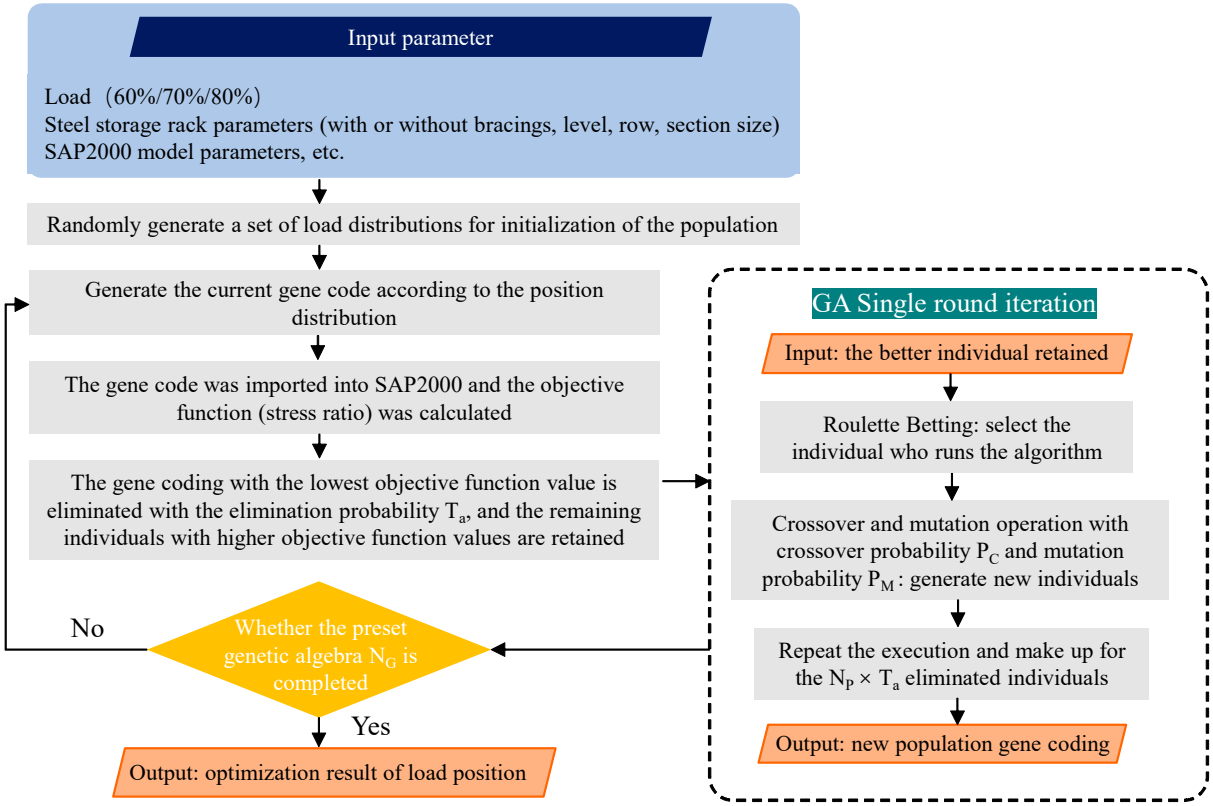

Figure 5. Flowchart of the program for GA.

Table 2. Related parameters in GA.

Parameter	Steel Storage Rack with Bracings	Steel Storage Rack without Bracings
Genetic algebra N_G	200	100
Population size N_P	150	150
Crossover probability P_C	0.65	0.65
Variation probability P_M	0.1	0.08
Elimination probability T_a	0.3	0.2

4. Optimization Analysis and Results

4.1. Analysis of Steel Storage Racks with Bracings

4.1.1. Optimization Results of the Most Unfavorable Load Distribution Pattern

The optimized results for the center of gravity, eccentricity, maximum stress ratio, and other related parameters under three different load rates are shown in Table 3. The optimization process and results for finding the most unfavorable load distribution pattern are shown in Figures 6–8. There are two curves in the GA tracking diagram. "The optimal maximum stress ratio of individual uprights" is the curve formed by the maximum stress ratio of the upright of the optimal individual (the most unfavorable distribution) among the 150 individuals (distribution patterns) in each generation. "The mean value of the maximum stress ratio of the population" is the curve formed by calculating and extracting the upright maximum stress ratio of each individual for the 150 distribution patterns represented by 150 individuals of each generation, and then the average of the 150 upright maximum stress ratios is obtained. "The most unfavorable distribution of load" is the most unfavorable load distribution pattern obtained through optimization, where the maximum stress ratio position is the most dangerous position, i.e., the control position of structural safety.

Table 3. Parameters related to the most unfavorable distribution patterns of the optimized loads.

Full Load Percentage	Center of Gravity—H	Eccentricity—P	Maximum Stress Ratio of Upright	Percentage Increase in Stress Ratio	Member Number
80%	6.00	0.29	1.214	18.4%	33
70%	5.90	0.36	1.153	12.5%	33
60%	5.67	−0.08	1.085	5.9%	21

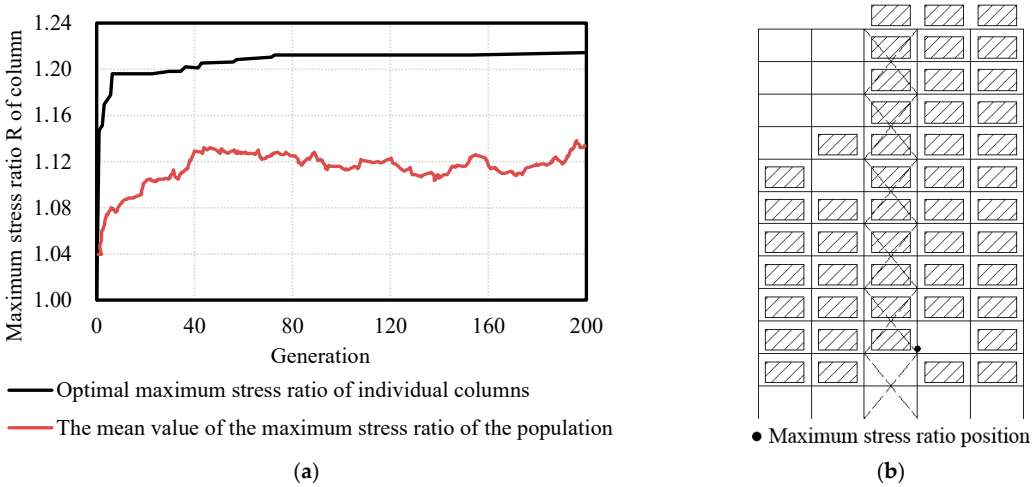

Figure 6. The most unfavorable distribution of load under 80% full load. (**a**) Tracking chart of optimization performance of GA. (**b**) The most unfavorable distribution of load (H = 6.00, P = 0.29).

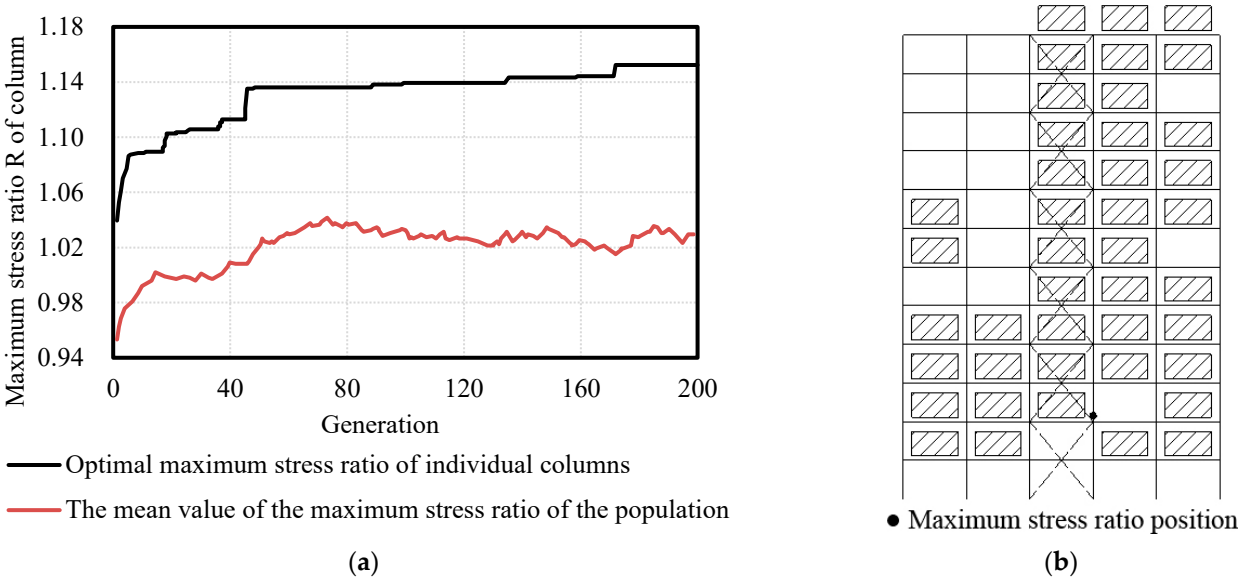

Figure 7. The most unfavorable distribution of load under 70% full load. (**a**) Tracking chart of optimization performance of GA. (**b**) The most unfavorable distribution of load (H = 5.90, P = 0.36).

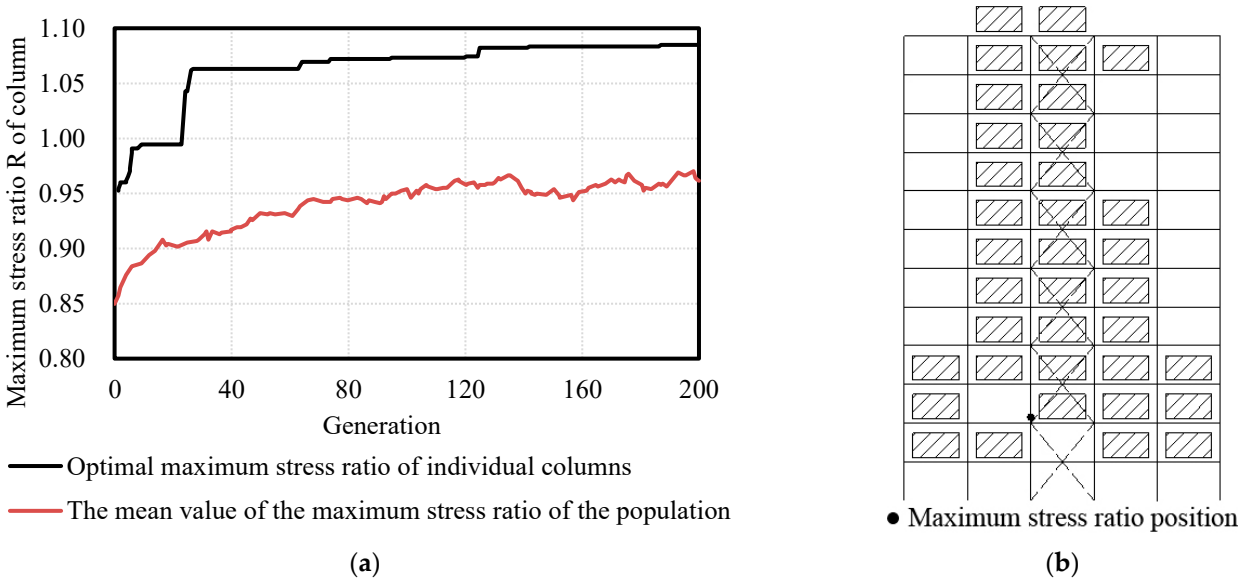

Figure 8. The most unfavorable distribution of load under 60% full load. (**a**) Tracking chart of optimization performance of GA. (**b**) The most unfavorable distribution of load (H = 5.67, P = −0.08).

From Table 3 and Figures 6–8, the following can be observed:

(1) Under 60%, 70%, and 80% of full load, the most unfavorable load distribution pattern obtained by the GA is neither the highest nor lowest center of gravity, and neither the largest nor smallest eccentricity, which further proves that judging the safety of the rack structure only by the height of the center of gravity and the size of the eccentricity is not accurate enough.

(2) Under 60%, 70%, and 80% of full load, the maximum stress ratios of the uprights with the most unfavorable load distribution pattern are 5.9%, 12.5%, and 18.4% higher than the full-load normal design, respectively, indicating that the load distribution pattern has a significant impact on the structural safety of steel storage racks.

(3) Under 60%, 70%, and 80% of full load, there are some commonalities in the optimization results of the most unfavorable load distribution patterns: The maximum stress

ratio appears in the two uprights of the spine bracing area, and they are all at the intersection of the short beam of the first level of spine bracing and the upright, while the corresponding load position is close to full load. The rest of the loads are mostly distributed at the bottom and the side row of the rack in the direction of the horizontal seismic force. The load distribution of the two load positions near the location of the maximum stress ratio is uneven, and the load position of the first level of the bracing area is empty.

4.1.2. Optimization Results of the Most Favorable Load Distribution Pattern

The optimized results for the center of gravity, eccentricity, maximum stress ratio, and other related parameters under three different load rates are shown in Table 4. The optimization process and results for finding the most favorable load distribution pattern are shown in Figures 9–11.

Table 4. Parameters related to the most favorable distribution patterns of the optimized loads.

Full Load Percentage	The Center of Gravity—H	Eccentricity—P	Maximum Stress Ratio of Upright	Member Number
80%	6.71	0.00	0.882	33
70%	6.24	0.05	0.777	35
60%	5.72	0.00	0.676	21

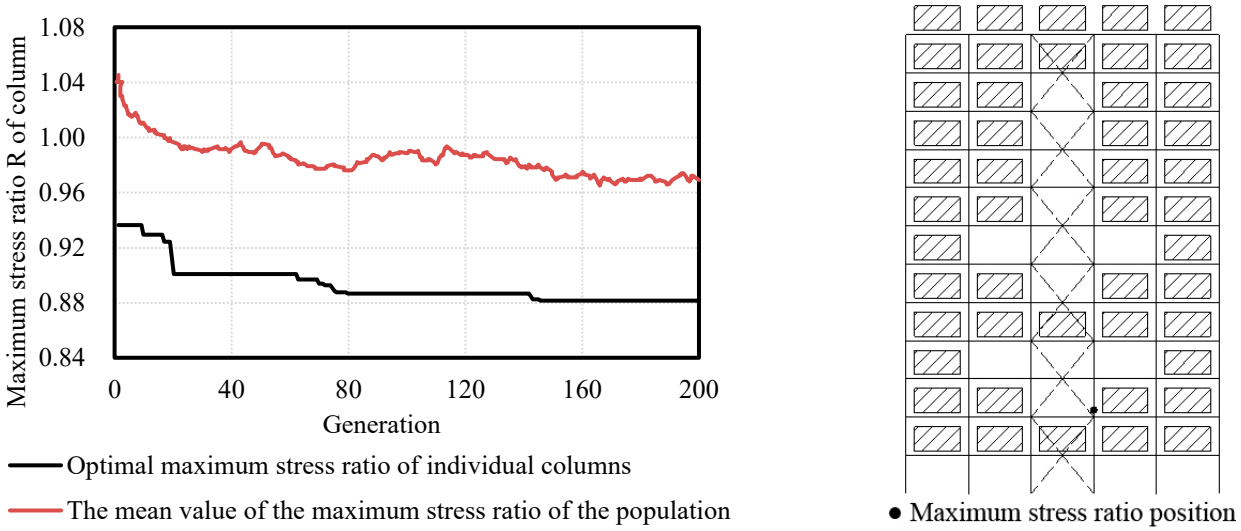

Figure 9. The most favorable distribution of load under 80% full load. (**a**) Tracking chart of optimization performance of GA. (**b**) The most favorable distribution of load (H = 6.71, P = 0).

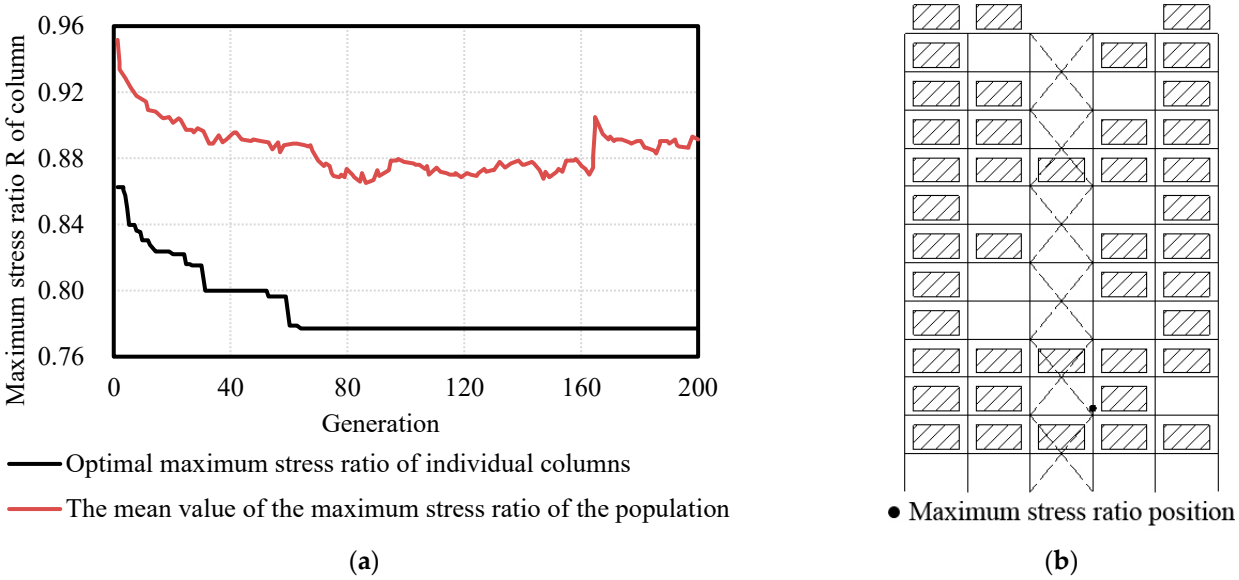

Figure 10. The most favorable distribution of load under 70% full load. (**a**) Tracking chart of optimization performance of GA. (**b**) The most favorable distribution of load (H = 6.24, P = 0.05).

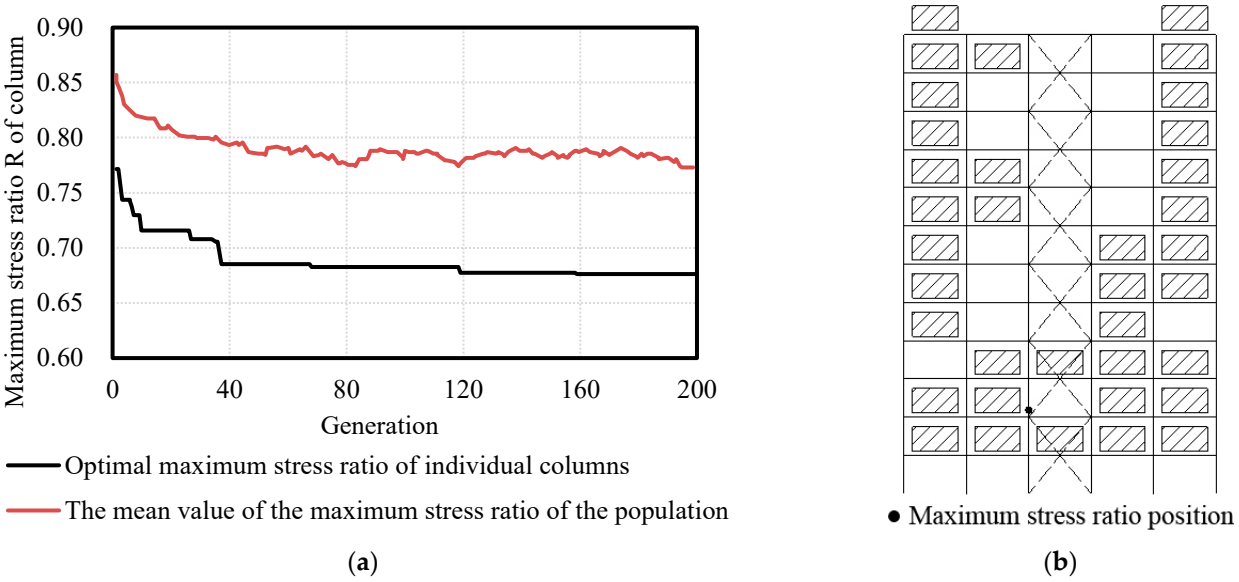

Figure 11. The most favorable distribution of load under 60% full load. (**a**) Tracking chart of optimization performance of GA. (**b**) The most favorable distribution of load (H = 5.72, P = 0).

From Table 4 and Figures 9–11, it can be seen that the optimization results of the most favorable load distribution patterns under three different load ratios have some commonalities: Very few loads are in the bracing area and empty load positions are located on the second level of the braced area. Most loads are in the two side columns and the distribution of load is symmetrical.

4.2. Analysis of Steel Storage Racks without Bracings

4.2.1. Optimization Results of the Most Unfavorable Load Distribution Pattern

The optimized results for the center of gravity, eccentricity, maximum stress ratio, and other related parameters under three different load rates are shown in Table 5. The optimization process and results for finding the most unfavorable load distribution pattern are shown in Figures 12–14.

Table 5. Parameters related to the most unfavorable distribution patterns of the optimized loads.

Full Load Percentage	The Center of Gravity—H	Eccentricity—P	Maximum Stress Ratio of Upright	Percentage Increase in Stress Ratio	Member Number
80%	2.81	0.00	1.121	19.1%	43
70%	2.86	−0.18	1.050	11.6%	83
60%	2.54	−0.79	0.993	5.5%	83

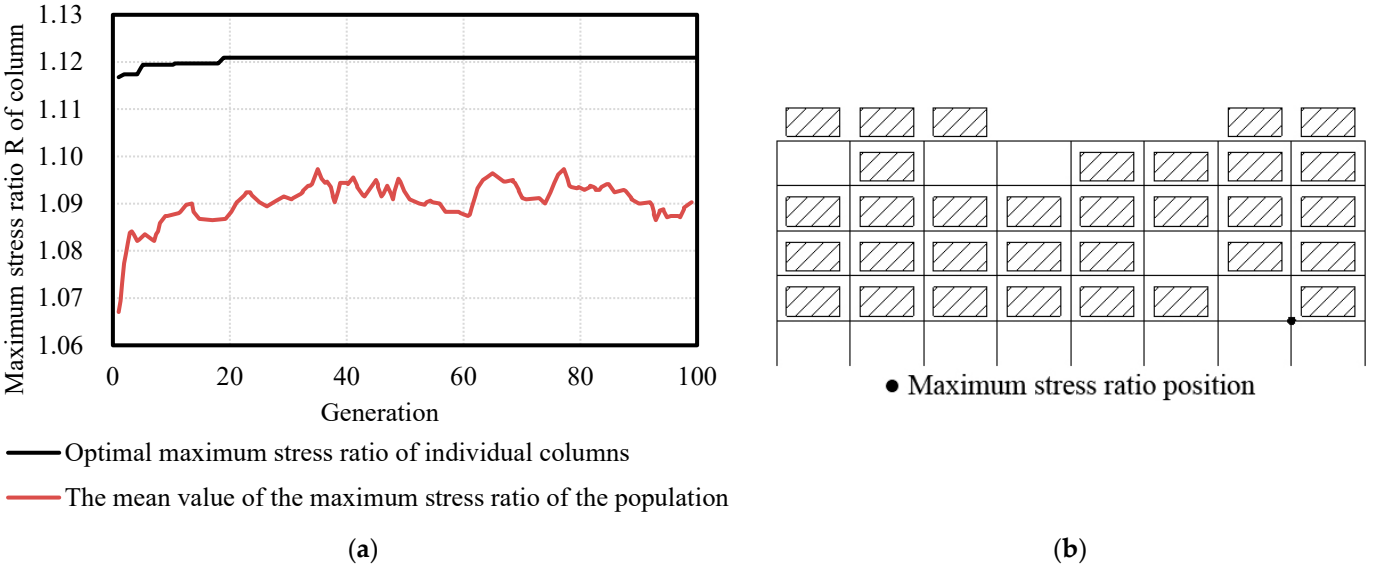

Figure 12. The most unfavorable distribution of load under 80% full load. (**a**) Tracking chart of optimization performance of GA. (**b**) The most unfavorable distribution of load (H = 2.81, P = 0.00).

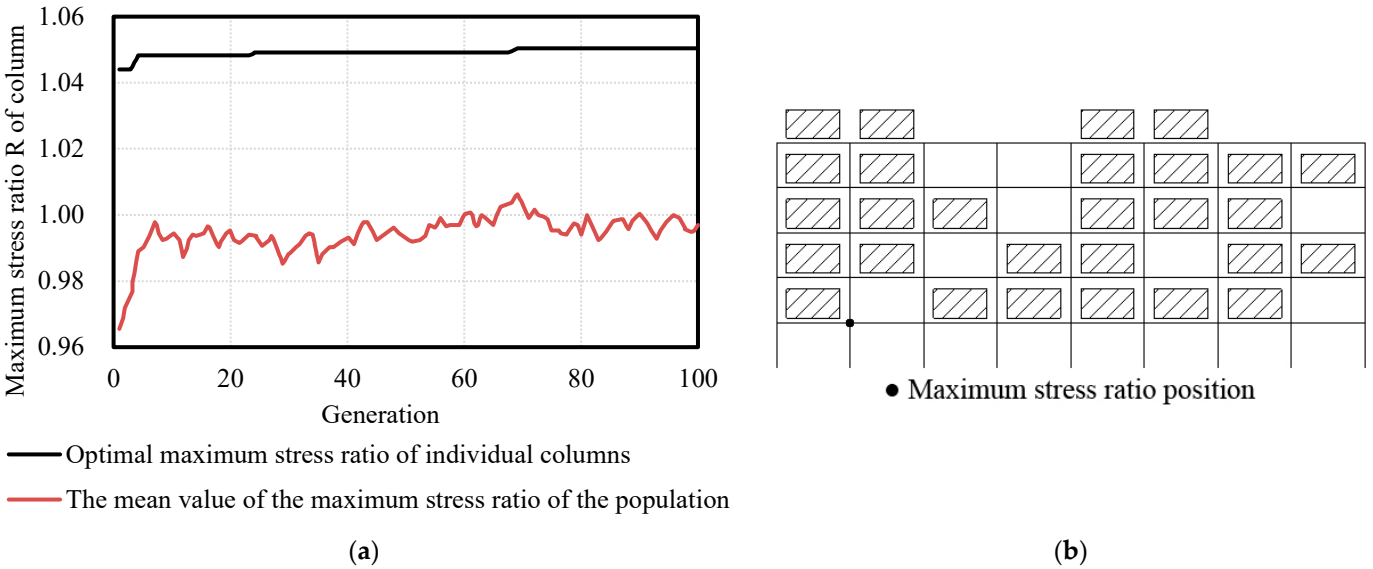

Figure 13. The most unfavorable distribution of load under 70% full load. (**a**) Tracking chart of optimization performance of GA. (**b**) The most unfavorable distribution of load (H = 2.86, P = −0.18).

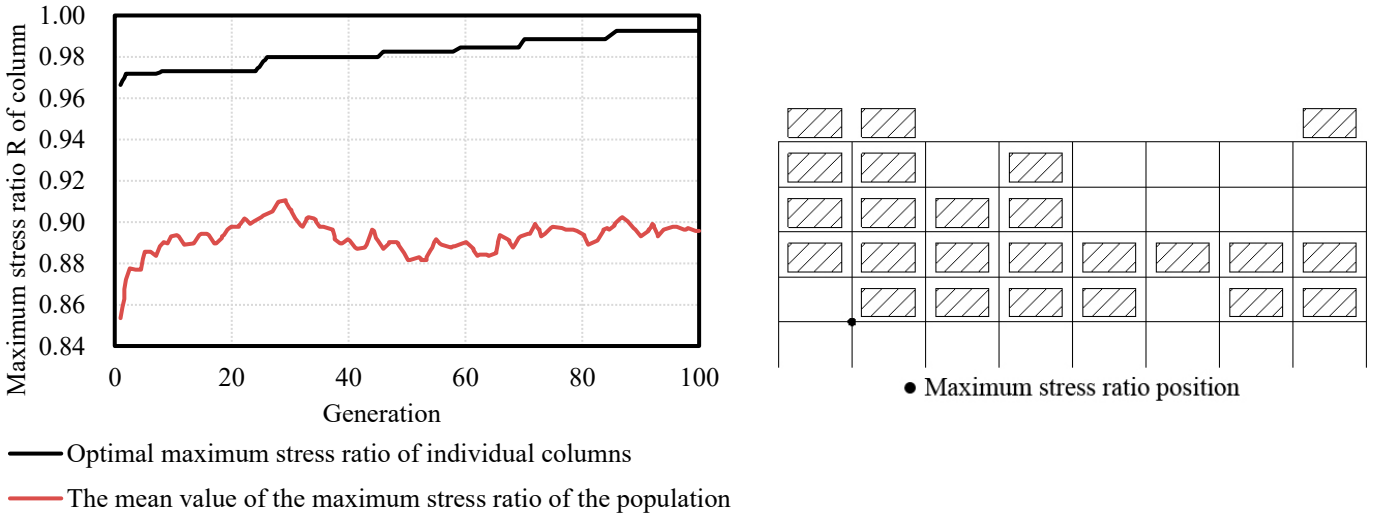

(**a**) (**b**)

Figure 14. The most unfavorable distribution of load under 60% full load. (**a**) Tracking chart of optimization performance of GA. (**b**) The most unfavorable distribution of load (H = 2.54, P = −0.79).

From Table 5 and Figures 12–14, the following can be seen:

(1) Under 60%, 70%, and 80% of full load, the center of gravity and eccentricity of the most unfavorable load distribution pattern generated by GA are neither the maximum nor the minimum, similar to the steel storage racks with bracings.
(2) Under 60%, 70%, and 80% of full load, the maximum stress ratios of the uprights with the most unfavorable load distribution pattern are 5.5%, 11.6%, and 19.1% higher than the full-load normal design, indicating that the distribution of load also has a significant impact on the structure of the steel storage racks without bracings.
(3) Under 60%, 70%, and 80% of full load, there are some commonalities in the optimization results of the most unfavorable load distribution patterns: the surrounding load position of the upright corresponding to the maximum stress ratio is basically fully loaded, and the load distribution at the joint of the first-level beam–upright of the upright corresponding to the maximum stress ratio is uneven.

4.2.2. Optimization Results of the Most Favorable Load Distribution Pattern

The optimized results for the center of gravity, eccentricity, maximum stress ratio, and other related parameters under three different load rates are shown in Table 6. The optimization process and results for finding the most favorable load distribution pattern are shown in Figures 15–17.

Table 6. Parameters related to the most favorable distribution patterns of the optimized loads.

Full Load Percentage	The Center of Gravity—H	Eccentricity—P	Maximum Stress Ratio of Upright	Member Number
80%	3.00	−0.06	0.955	25
70%	2.68	0.07	0.819	83
60%	2.83	0.00	0.717	1

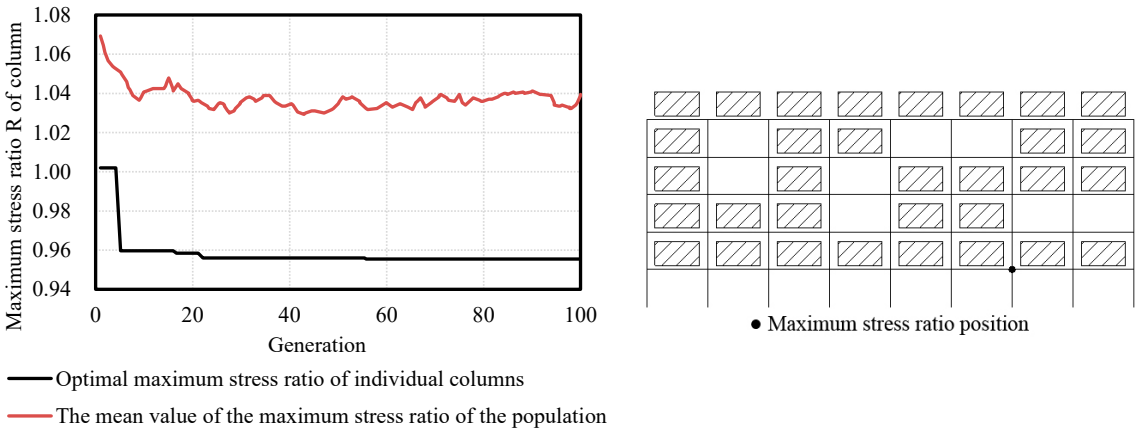

(**a**) (**b**)

Figure 15. The most favorable distribution of load under 80% full load. (**a**) Tracking chart of optimization performance of GA. (**b**) The most favorable distribution of load (H = 2.68, P = 0.07).

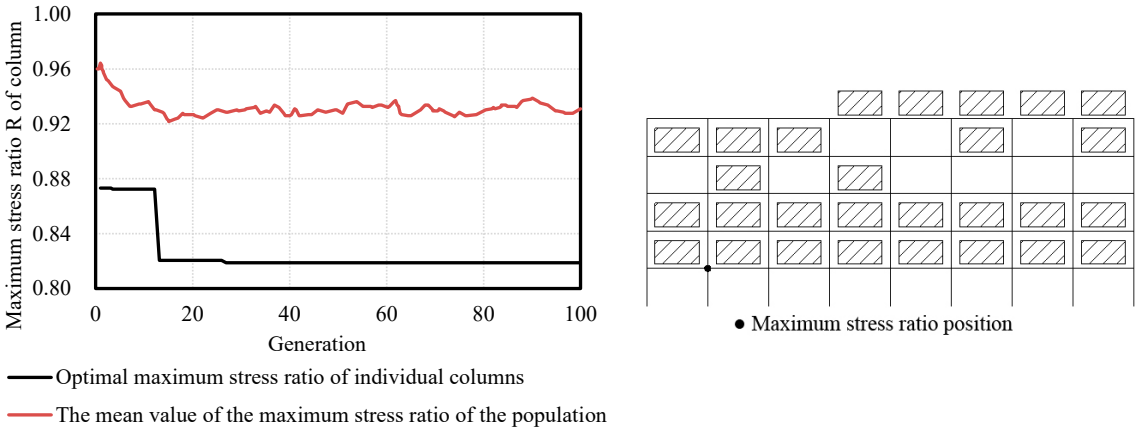

(**a**) (**b**)

Figure 16. The most favorable distribution of load under 70% full load. (**a**) Tracking chart of optimization performance of GA. (**b**) The most favorable distribution of load (H = 2.68, P = 0.07).

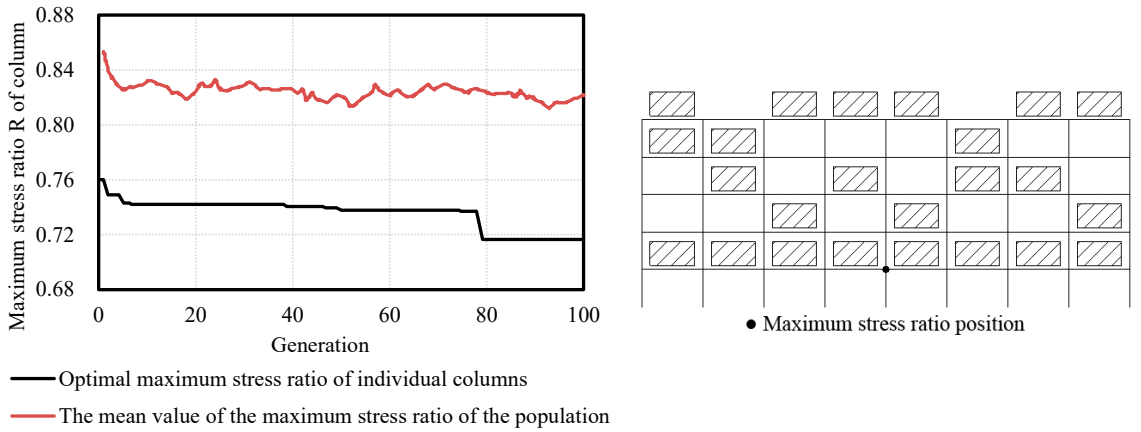

(**a**) (**b**)

Figure 17. The most favorable distribution of load under 60% full load. (**a**) Tracking chart of optimization performance of GA. (**b**) The most favorable distribution of load (H = 2.83, P = 0.00).

From Table 6 and Figures 15–17, the following can be seen:

(1) Under 60%, 70%, and 80% of full load, all loads are evenly distributed in each upright, and the number of loads carried by each upright is basically the same. For example, each upright in Figure 15 basically carries eight loads.
(2) Under 60%, 70%, and 80% of full load, the load located on the first level is fully loaded, and there is no uneven distribution of load at the position of the maximum stress ratio (beam–upright joint on the first level).

4.3. Summary of Load Distribution Patterns

In Sections 4.1 and 4.2, the most favorable and unfavorable load distribution patterns for braced and unbraced racks are obtained, respectively. This section summarizes and discusses the results. From Tables 3–6 and Figures 6–17, the following can be observed:

(1) Under 60%, 70%, and 80% of full load, the most unfavorable load distribution pattern obtained by the GA is neither the highest or the lowest center of gravity, nor the maximum or the minimum eccentricity. With the most unfavorable load distribution pattern (partially loaded), the maximum stress ratio of the upright is higher than that of the full-load normal design for both the racks with and without bracings. This indicates that it is unreasonable to evaluate the safety of the rack only by the height of the center of gravity, eccentricity, or total load, and that the load distribution pattern has a significant impact on the structural safety of the rack.
(2) Under 60%, 70%, and 80% of full load, the load position around the upright with the maximum stress ratio of the most unfavorable load distribution pattern obtained by the GA is basically fully loaded near those uprights for both the racks with and without bracings.
(3) It can be seen from the most favorable load distribution pattern that the first row is fully loaded for both the racks with and without bracings. The most favorable load distribution pattern of the braced or unbraced rack have basically the same load in each column because the evenly distributed load can make the upright produce a lower stress ratio. For the braced rack, the uprights on the two side columns bear the main load, and there are few loads in the braced area. Because the stiffness of the braced area is high, it will bear more load and have a higher stress ratio, so reducing the axial force of the column in the braced area will make the stress ratio of the upright lower.

5. Load Distribution Pattern

5.1. Detailed Analysis

In the previous section, in addition to the final distribution pattern obtained from the optimization, a large number of load distribution patterns are generated and calculated during the optimization process. If the stress ratio limit is determined as the maximum stress ratio of the upright under full load (1.025 for steel storage racks with bracings and 0.941 for steel storage racks without bracings), then the load distribution patterns generated during the optimization process will be divided into two groups: over-limit and within-limit distribution patterns. Then, the statistical analyses on the two groups of distribution patterns are processed separately to obtain the contours of the probability distribution of over-limit and within-limit loads.

Take the over-limit distribution pattern as an example. First, remove the duplicated distribution patterns in the group. Then, the maximum stress ratio of the upright corresponding to each distribution pattern in the group is used as its weighted value. The higher the upright maximum stress ratio is, the greater the weight of its corresponding load distribution pattern is, and the greater the influence is. Then, all the weighted distribution patterns in the group are counted, and the number of times N that a load appears at each load position is obtained. Finally, normalization is performed, and the probability value of the load position with the least number of load occurrences is designated as 0 (dark blue) and the probability value of the load position with the greatest number of load occurrences is designated as 1 (dark red). Therefore, the closer the color of the load position is to dark

red, the more loads appear in this position. Contrarily, the closer it is to dark blue, the less loads appear. When probability statistics are analyzed for the within-limit group, the maximum stress ratio of the upright corresponding to each distribution pattern is used as its weighted value.

5.2. Steel Storage Racks with Bracings Load Distribution Pattern

5.2.1. Contours of Probability Distribution of Over-Limit Load

The distribution pattern of the over-limit load generated during the optimization of the steel storage racks with bracings in Section 4.1.1 from probability statistics form the probability distribution contours, as shown in Figure 18.

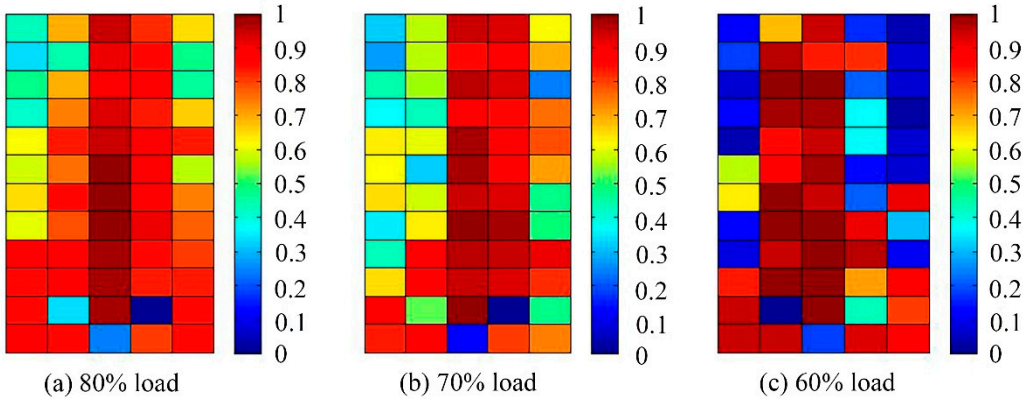

Figure 18. Probability distribution contours of the over-limit load.

Figure 18a,c are compared with the load distribution patterns obtained from the optimization in Figures 6–8, respectively. It can be seen that the probability distribution contours have similarities with the most unfavorable way of load distribution finally obtained by optimization, which further proves the reliability of the load level genetic optimization algorithm and that the commonality of the unfavorable way of load distribution with the steel storage racks with bracings summarized in Section 4.1.1 is correct. According to Figure 18 and the commonness of adverse distribution modes of load on the braced racking systems, the distribution risk mode of load on the braced racking systems is determined. As shown in Figure 19, it is defined as a "convex" distributed hazardous mode.

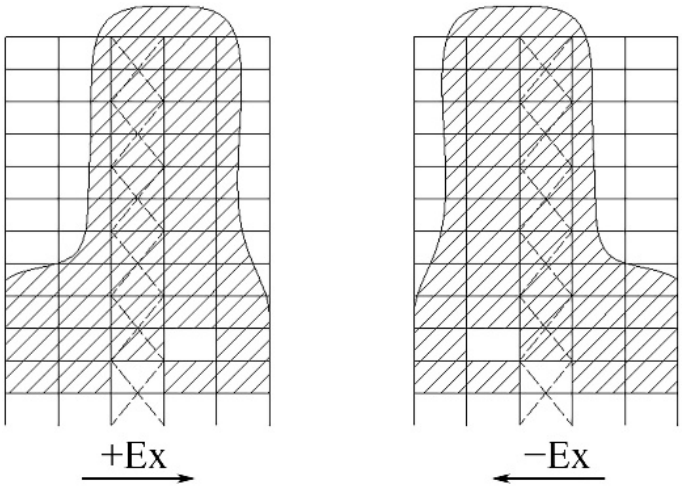

Figure 19. Load distribution hazard model for steel storage racks with bracings.

5.2.2. Contours of Probability Distribution of Within-Limit Load

The distribution pattern of the within-limit load generated during the optimization of steel storage racks with bracings in Section 4.1.2 from the probability statistics form the probability distribution contours, as shown in Figure 20.

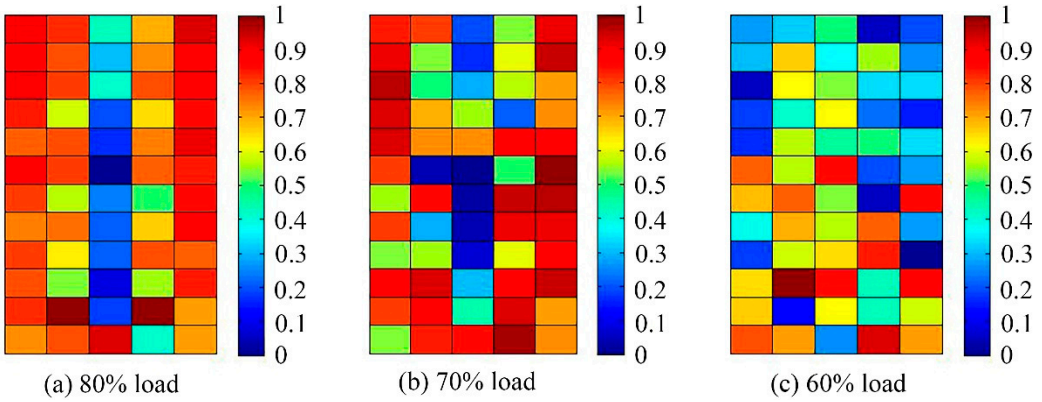

Figure 20. Load distribution hazard models for the steel storage racks with bracings.

Figure 20a,c are compared with the load distribution methods obtained from the optimization in Figures 9–11, respectively. It can be seen that the probability contours under 80% and 70% load are very close to the most favorable distribution modes finally obtained by optimization. However, the probability contours with 60% load are not very regular. The reason is that there are too many distribution modes that do not exceed the limit under a 60% load rate. Many distribution modes that do not exceed the limit do not conform to the distribution commonness summarized in Section 4.1.2 as the load is too small. The distribution safe mode of load on the steel racks with bracings is summarized as shown in Figure 21. It is defined as a "concave" distributed safe mode.

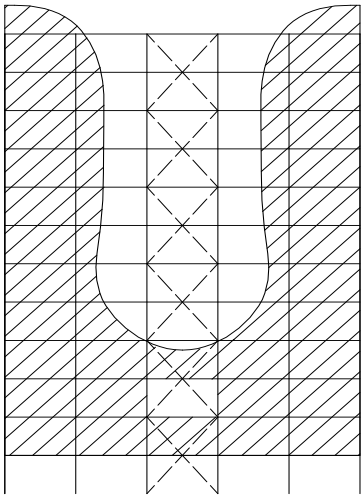

Figure 21. Danger model of load distribution on the steel storage racks with bracings.

5.3. Steel Storage Racks without Bracings Load Distribution Pattern

5.3.1. Contours of Probability Distribution of Over-Limit Load

Probability statistical processing was carried out on the over-limit load distribution mode generated in the optimization process of the steel racks without bracings to form the probability distribution contours, as shown in Figure 22.

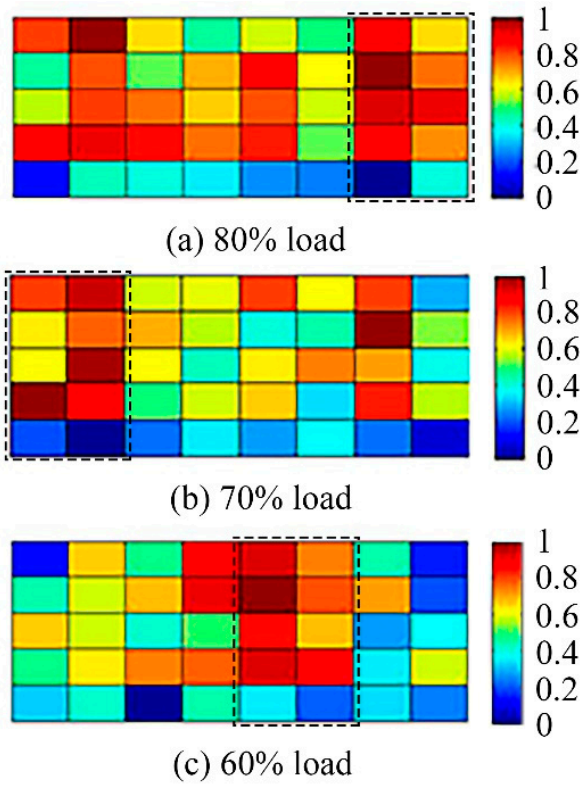

Figure 22. Probability distribution contours of the over-limit load.

It can be seen from Figure 22 that there are no strong regularities in the probability distributions of the steel storage racks without bracings in the over-limit group. The reason is that steel storage racks without bracings are different from the steel storage racks with bracings. There is no bracing system, and the horizontal seismic force is evenly distributed to each row. According to the analysis of the results in Section 4.2.1, it can be concluded that: If two uprights are carrying the same load at the 10 positions, the stress ratios of the two uprights are similar to each other. Therefore, the maximum stress ratio may occur at each of the uprights. Regarding the comparison of the three load distribution modes shown in Figure 22 under 80% load, except for the load on the solid line in the figure, the other loads are randomly distributed on the dotted line. The comparison results are shown in Table 7 and Figure 23.

Table 7. Relations between the distribution mode of load and the stress of the upright.

The Manner in Which Loads Are Distributed	a	b	c
Position of maximum stress ratio	At the beam–upright joint of the first level		
Maximum stress ratio	1.116	1.111	1.130
Total horizontal seismic force (kN)	11.3	11.3	25.3
The stress ratio due to the axial force N	0.332	0.332	0.332
Stress ratio due to Mx [1] (not the axis of symmetry)	0.005	0.001	0.001
Stress ratio due to My [1] (axis of symmetry)	0.779	0.778	0.796
Maximum stress ratio	1.116	1.111	1.130
Total horizontal seismic force (kN)	11.3	11.3	25.3

[1] Mx and My are the biaxial bending moment values calculated in SAP2000 for each member of the rack model, which can be used to further calculate the stress ratio of the member.

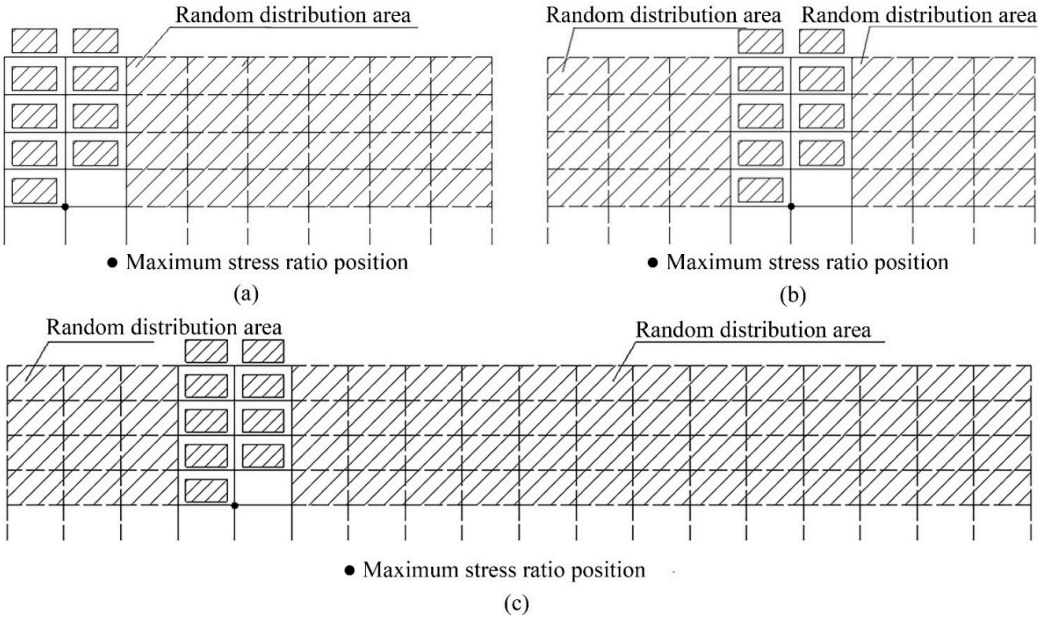

Figure 23. Comparison of three distribution modes of load. (**a**) "Right convex" mode of load distribution appears at the edge of rack. (**b**) "Right convex" mode of load distribution appears at the middle of rack. (**c**) "Right convex" mode of load distribution appears at the other positions of rack.

As can be seen from Table 7, the results of the three distribution modes are very similar, so it can be suggested that the distribution risk model of load with the steel storage racks without bracings shown in Figure 24 should be avoided. The pattern of load distribution shown in Figure 24 is defined as a "right convex" mode of load distribution. In the normal use of steel storage racks without bracings, a warning should be issued if an upright has a "right convex" distribution of load.

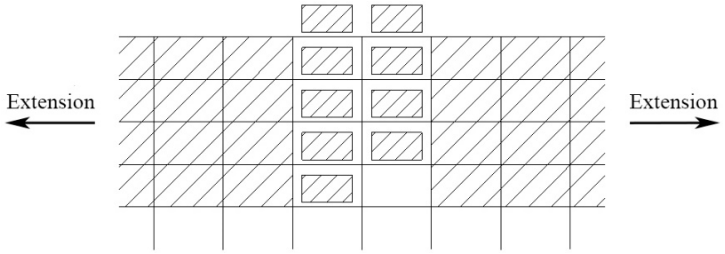

Figure 24. Hazard model of load distribution on steel storage racks without bracings.

5.3.2. Contours of Probability Distributions of the Within-Limit Load

The probability distribution patterns of the valid load generated during the optimization of steel storage racks without bracings were statistically processed to form probability distribution contours. However, the maximum stress ratio of the upright under 80% load on the steel storage racks without bracings is higher than that under full load (0.941). Therefore, only the probability distribution contours for 70% and 60% of load are listed, as shown in Figure 25.

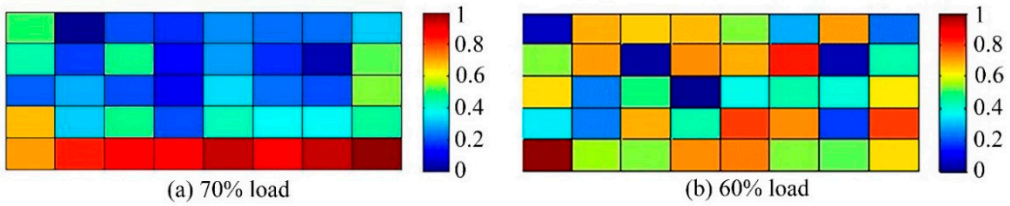

Figure 25. Contours of probability distribution of the unexpired load.

For steel storage racks without bracings, it can be seen from Figure 25 that the regularities of the probability distributions of the within-limit load are also weak. The reason is the same as the probability distribution of the over-limit load. Nonetheless, the figure reveals that the chance of load occurrence on the first level is rather high, particularly when the load is relatively substantial (70%). This is the reason to avoid uneven distribution of load in the first tier when optimizing for the most favorable distribution pattern of load.

There is no specific load distribution safety mode for steel storage racks without bracings, but it conforms to the commonalities summarized in Figure 25. The characteristics of the load distribution safety mode are described as follows: the load is evenly distributed in each row, and there is no uneven distribution in the first level.

6. Conclusions

The load distribution on the rack structures could pose many risks during a seismic event. This study utilized the stochastic optimization algorithms such as the genetic algorithm to assess the most unfavorable and favorable load distributions by diverting from the conventional speculation. After 200 and 100 generations in the GA, the most unfavorable and favorable load distributions of the rack under 60%, 70%, and 80% of full load were identified, and their statistical summaries were drawn from the optimized results from each generation. These optimization results confirmed that the maximum stress ratio of the upright under the most unfavorable load distribution is higher than that under full load for both the steel storage racks with bracing or not. Therefore, the traditional speculation of full load (with a higher center of gravity) is not the worst loading case. Moreover, for the braced rack, the uprights in the spine bracing area are the critical upright, and the maximum stress ratio is located at the junction of the upright and the short beam supported on the first level. On the other hand, the maximum stress ratio of the steel storage rack without bracings is located at the joint between the upright and the first-level beam, which is a consistent observation from the optimization. Furthermore, from the statistical summary of the optimization results, the "convex" load distribution is bad for the racks with bracings, designated as the hazardous mode, while the "concave" load distribution is the safe mode. For the racks without bracings, the "right convex" load distribution is the hazardous mode, and no specific load distribution is identified as the safe mode. Finally, this study provides a new and feasible idea for studying the impact of load distribution on the seismic performance of steel storage racks. In future studies, it is worth expanding the scope to include all possible buckling states, since the study here is limited to local and global buckling and a non-binary loading assumption at the load position.

Author Contributions: Conceptualization, T.D., Y.N., L.Y. and Z.L. (Zhanjie Li); methodology, T.D., Y.N., Z.L. (Zhiqiang Lin) and Z.L. (Zhanjie Li); software, Z.L. (Zhiqiang Lin); validation, T.D. and L.Y.; formal analysis, T.D. and Y.N.; investigation, T.D., Y.N. and Z.L. (Zhiqiang Lin); resources, Z.L. (Zhiqiang Lin); data curation, T.D. and Z.L. (Zhiqiang Lin); writing—original draft preparation, T.D.; writing—review and editing, Y.N., L.Y. and Z.L. (Zhanjie Li); visualization, Y.N. and Z.L. (Zhqiang Lin); supervision, L.Y.; project administration, L.Y.; funding acquisition, L.Y. All authors have read and agreed to the published version of the manuscript.

Funding: This research was funded by National Natural Science Foundation of China grant number 52278150 and Central Government for Local Science and Technology Development of Tibetan Autonomous Region grant number XZ202201YD0032C and Natural Science Foundation of Jiangsu grant number BK20191268.

Institutional Review Board Statement: Not applicable.

Informed Consent Statement: Not applicable.

Data Availability Statement: The data are available upon request from the corresponding authors.

Acknowledgments: The research was sponsored by the National Natural Science Foundation of China (Grant No. 52278150), the Project of Central Government for Local Science and Technology

Development of Tibetan Autonomous Region (Grant No. XZ202201YD0032C), and the Natural Science Foundation of Jiangsu (Grant No. BK20191268).

Conflicts of Interest: The authors declare no conflict of interest.

References

1. Zhao, X.; Ren, C.; Qin, R. An experimental investigation into perforated and non-perforated steel storage rack uprights. *Thin Walled Struct.* **2017**, *112*, 159–172. [CrossRef]
2. Talebian, N.; Gilbert, B.P.; Miller, D.; Karampour, H. Biaxial bending design of solid steel storage rack uprights in global buckling. *J. Constr. Steel Res.* **2022**, *196*, 107395. [CrossRef]
3. Ren, C.; Wang, B.; Zhao, X. Numerical predictions of distortional-global buckling interaction of perforated rack uprights in compression. *Thin Walled Struct.* **2019**, *136*, 292–301. [CrossRef]
4. Maguire, J.R.; Teh, L.H.; Clifton, G.C.; Lim, J.B.P. Residual capacity of cold-formed steel rack uprights following stomping during rocking. *J. Constr. Steel Res.* **2019**, *159*, 189–197. [CrossRef]
5. Bonada, J.; Pastor, M.M.; Roure, F.; Casafont, M. Distortional influence of pallet rack uprights subject to combined compression and bending. *Structures* **2016**, *8*, 275–285. [CrossRef]
6. Yin, L.; Tang, G.; Zhang, M.; Wang, B.; Feng, B. Monotonic and cyclic response of speed-lock connections with bolts in storage racks. *Eng. Struct.* **2016**, *116*, 40–55. [CrossRef]
7. Yin, L.; Tang, G.; Li, Z.; Zhang, M.; Feng, B. Responses of cold-formed steel storage racks with spine bracings using speed-lock connections with bolts I: Static elastic-plastic pushover analysis. *Thin Walled Struct.* **2018**, *125*, 51–62. [CrossRef]
8. Yin, L.; Tang, G.; Li, Z.; Zhang, M. Responses of cold-formed steel storage racks with spine bracings using speed-lock connections with bolts II: Nonlinear dynamic response history analysis. *Thin Walled Struct.* **2018**, *125*, 89–99. [CrossRef]
9. Dai, L.; Zhao, X.; Rasmussen, K.J.R. Flexural behaviour of steel storage rack beam-to-upright bolted connections. *Thin Walled Struct.* **2018**, *124*, 202–217. [CrossRef]
10. Dai, L.; Zhao, X.; Rasmussen, K.J.R. Cyclic performance of steel storage rack beam-to-upright bolted connections. *J. Constr. Steel Res.* **2018**, *148*, 28–48. [CrossRef]
11. Escanio, L.A.; Elias, G.C.; de Almeida Neiva, L.H.; Alves, V.N.; Sarmanho, A.M.C. Analysis of beam-to-upright end connections steel storage systems. *Adv. Steel Constr.* **2020**, *16*, 279–286. [CrossRef]
12. Zhao, X.; Dai, L.; Rasmussen, K.J.R. Hysteretic behaviour of steel storage rack beam-to-upright boltless connections. *J. Constr. Steel Res.* **2018**, *144*, 81–105. [CrossRef]
13. Shariati, M.; Tahir, M.M.; Wee, T.C.; Shah, S.N.R.; Jalali, A.; Abdullahi, M.a.M.; Khorami, M. Experimental investigations on monotonic and cyclic behavior of steel pallet rack connections. *Eng. Fail. Anal.* **2018**, *85*, 149–166. [CrossRef]
14. Tagliafierro, B.; Montuori, R.; Castellano, M.G. Shake table testing and numerical modelling of a steel pallet racking structure with a seismic isolation system. *Thin Walled Struct.* **2021**, *164*, 107924. [CrossRef]
15. Shaheen, M.S.A.; Rasmussen, K.J.R. Seismic tests of drive-in steel storage racks in cross-aisle direction. *J. Constr. Steel Res.* **2019**, *162*, 105701. [CrossRef]
16. Sajja, S.R.; Beale, R.G.; Godley, M.H.R. Shear stiffness of pallet rack upright frames. *J. Constr. Steel Res.* **2008**, *64*, 867–874. [CrossRef]
17. Maguire, J.R.; Teh, L.H.; Clifton, G.C.; Tang, Z.; Lim, J.B. Cross-aisle seismic performance of selective storage racks. *J. Constr. Steel Res.* **2020**, *168*, 105999. [CrossRef]
18. RMI. *Specification for the Design, Testing and Utilization of Industrial Steel Storage Racks*; Rack Manufacturers Institute: Charlotte, NC, USA, 2008.
19. *AS 4084*; Steel Storage Racking. Standards Australia: Sydney, Australia, 1993.
20. *EN15512*; Steel Static Storage Systems—Adjustable Pallet Racking Systems—Principles for Structural Design. European Committee for Standardization: Belgium, Brussels, 2009.
21. Coutinho, G.E.N.R. *Numerical Simulation of the Seismic Behavior of Steel Storage Pallet Racking Systems*; Universidadetecnica De Lisboa: Lisbon, Portugal, 2008.
22. Beale, R.G.; Godley, M.H.R. The design of the pallet program. In Proceedings of the International Specialty Conference on Cold-Formed Steel Structures, Orlando, FL, USA, 17–18 October 2002; pp. 353–368.
23. Beale, R.G.; Godley, M.H.R. Developments in the pallet program. In Proceedings of the International Conference on Advances in Structures, Steel, Concrete, Composite and Aluminium, Sydney, Australia, 22–25 January 2003; pp. 237–243.
24. Al Qarud, F.; Shatnawi, A.; Abdel-Jaber, M.S.; Beale, R.G. Influence of partial loading on the behaviour of pallet rack structures. *Adv. Steel Constr.* **2010**, *6*, 619–634. [CrossRef]
25. Petrovčič, S.; Kilar, V. Effects of horizontal and vertical mass-asymmetric distributions on the seismic response of a high-rack steel structure. *Adv. Struct. Eng.* **2012**, *15*, 1977–1988. [CrossRef]
26. Michalewicz, Z. *Genetic Algorithms + Data Structures = Evolution Programs*; Springer: New York, NY, USA, 1996.
27. Yang, S.; Shi, M.; Zhang, Q.; Yu, Y.; Zhou, Y.; Li, X. The optimization of slotting based on the power drive-through rack. In Proceedings of the 2nd International Conference on Applied Mechanics and Materials (ICAMM 2013), Zhuhai, China, 23–24 November 2013; p. 1537.

28. Zhu, J.; Zhang, W.; Xue, F. Storage location assignment optimization of stereoscopic warehouse based on genetic simulated annealing algorithm. *J. Comput. Appl.* **2020**, *40*, 284–291.
29. *CECS 23-1990*; The Specification for Design of Steel Storage Racks. China Association for Engineering Construction Standardization: Beijing, China, 1990. (In Chinese)
30. *GB 50018-2002*; Technical Code of Cold-Formed Thin-wall Structures. China Ministry of Construction: Beijing, China, 2002. (In Chinese)
31. *GB 50011–2010*; Code for Seismic Design of Buildings. China Ministry of Construction: Beijing, China, 2016. (In Chinese)
32. Tang, G.; Cheng, W.; Yin, L.; Lin, Z.; Ma, M. Research on the effect of gravity center and eccentricity on the seismic behavior of steel storage racks. *Prog. Steel Build. Struct.* **2018**, *20*, 54–62. (In Chinese) [CrossRef]
33. *GB/T 700-2006*; Carbon Structural Steels. China Standard Press: Beijing, China, 2006. (In Chinese)
34. Deb, K. An efficient constraint handling method for genetic algorithms. *Comput. Methods Appl. Mech. Eng.* **2000**, *186*, 311–338. [CrossRef]
35. Deb, K.; Kumar, A. Real-coded genetic algorithms with simulated binary crossover: Studies on multimodal and multiobjective problems. *Complex Syst.* **1995**, *9*, 431–454.